Structure and Reactivity of Rice Husk Chars under Different Bulk Densities

Bichen Liu,[a,b] Qizhou Fan,[a,b,]* Wei Wu,[a,b] and Yujie Hu [a,b]

The effects of bulk density on the structure and combustion characteristics of rice husk (RH) char were studied under isothermal conditions. The char from each reaction stage was obtained through pyrolysis of RH/Al_2O_3. Thermogravimetric-Fourier transform infrared analysis was used to study the release of gaseous products during the fine particle pyrolysis of RH/Al_2O_3. The results showed that the bulk density of the particles seriously affected the release rate and product distribution of gaseous products during pyrolysis, especially in the release phase of volatiles. In comparison, biomass pellets had a faster pyrolysis reaction rate at low bulk densities, which resulted in lower contents of O and H in the char obtained at this stage, and the aromatic structure content slowly increased. In the carbonization stage, the low bulk density promoted the increase in surface area and pore volume expansion of char. The degree of aromatization in char was higher, but the carbon content decreased. The addition of Al_2O_3 limited the growth of aromatic crystallites, while the char obtained at high bulk density tended to be graphitized. The char reactivity at the two bulk densities first decreased and then slightly increased, but the char obtained at high bulk density had better combustion reactivity.

Keywords: Biomass; Pyrolysis; Fixed bed; Char structure; Reactivity

Contact information: a: College of Engineering, Huazhong Agricultural University, No. 1, Shizishan Street, Hongshan District, Wuhan, 430070, Hubei Province, P. R. China; b: Key laboratory of Agricultural Equipment in the Mid-lower Yangtze River, Ministry of Agriculture, Wuhan, 430070, Hubei Province, P. R. China; **Corresponding author: qizhoufan@mail.hzau.edu.cn*

INTRODUCTION

With the overuse of fossil fuels and concerns about environmental protection, the research and use of bioenergy technology has attracted worldwide attention. Agricultural waste is one of the most extensive renewable energy sources outside of fossil fuel energy. Biomass can be converted into high-grade energy sources, such as combustible gas and biochar, through pyrolysis. Biochar produced by pyrolysis is rich in organic carbon, porosity, alkaline, and other properties (Chandra and Bhattacharya 2019). Biochar can be used for multi-purpose materials such as soil improvers, carbon-based compound fertilizers, and organic dye adsorbents. Biomass pyrolysis carbonization technology can achieve high value utilization of biomass and mitigate the negative impacts of greenhouse gases and environmental pollution (Cataldo *et al.* 2018; Lateef *et al.* 2019).

Countries around the world have made some progress in pyrolysis carbonization technology. The existing research mainly focuses on the pyrolysis characteristics, the physical and chemical properties of char, the potential utilization of char, and the energy loss of carbonization (Yi *et al.* 2016; Jian *et al.* 2019; Rizzo *et al.* 2019). However, the key of biomass pyrolysis is the pyrolysis reaction process.

Pyrolysis temperature, holding time, and heating rate have been the hotspots of such research (Burhenne *et al.* 2013; Klinger *et al.* 2018; Zhao *et al.* 2018). Thines *et al.* (2017) studied the effect of pyrolysis parameters on the structure of durian char, where the pyrolysis temperature was between 500 and 900 °C, and the reaction time was between 10 min and 30 min. The char yield changed noticeably in the range 700 °C to 900 °C for 25 min to 30 min. The specific surface area first increased and then decreased with the increase in reaction time. The maximum specific surface area was achieved at lower temperatures as the pyrolysis time increased. The study performed by Pehlivan *et al.* (2017) obtained a maximum char yield of 31.25% at a pyrolysis temperature of 400 °C, N_2 flow rate of 100 cm^3/min, heating rate of 10 °C/min, and an average particle size of 1.18 mm. In conclusion, the temperature, holding time, and heating rate all affect the pyrolysis process.

Studies have shown that the size of the biomass particles themselves is large, which leads to a slow heat transfer and mass transfer inside the particles. At the same time, the particles are rich in biomass and difficult to break, and their initial accumulation condition has a huge impact on the pyrolysis and carbonization process. Atreya *et al.* (2017) studied the pyrolysis of anhydrous wood samples of various sizes (5 mm to 20 mm) and shapes (spheres, cylinders, cubes, and rectangular blocks) using a vertical tube furnace experiment. Fine particles are pyrolyzed faster at elevated temperatures, producing less char and more volatile compounds. Pimenta *et al.* (2018) studied the effect of wood bulk density on oxidative pyrolysis in a downdraft continuous fixed bed reactor. The oxidation zones were uniform in the wood particle combustion bed with three times the packing density, but there were differences in the chip bed of low density. The structure and reactivity of biomass pyrolysis and carbonization are complex. Biagini *et al.* (2009) studied the effects of char structure morphology under rapid heating conditions. They found that biomass particles undergo plastic deformation during rapid pyrolysis and affect char structure and char reactivity. At the same time, the characteristics of the char particles themselves are related to the utilization of biomass. Azuara *et al.* (2015) found that γ-Al_2O_3 is beneficial to the increase of sludge pyrolysis liquid product. The Al_2O_3 is mostly used as a support carrier. From these studies, it is known that the bulk density of the biomass particles affects the pyrolysis reaction rate, the char structure, and the supported catalyst to enhance the liquid phase product.

At present, many countries in the world have conducted extensive research on biomass pyrolysis technology, but the core of pyrolysis is the pyrolysis reaction process. Because the pyrolysis reaction process of biomass particles is extremely complicated, it is difficult to distinguish the influence of bulk density on the reaction mechanism of the pyrolysis process solely by the accumulation of biomass particles. Therefore, adding physical barriers to biomass particles to simulate the pyrolysis reaction of biomass particles under different bulk densities is a pressing area of study.

In the usual case, Al_2O_3 particles are used as catalyst support carriers for the study of pyrolysis liquid products, but few studies are performed on solid products. Therefore, in this paper, the mixed pyrolysis of Al_2O_3 and biomass particles was studied to simulate pyrolysis char prepared by biomass at different bulk densities. The functional groups, crystallite structure, pore structure, and char reactivity of pyrolysis char in each reaction stage were analyzed. This study aimed to improve pyrolysis carbonization technology and the high value utilization of biomass.

EXPERIMENTAL

Materials

The experiment used a typical agricultural biomass sample, rice husk (RH) (Huazhong Agricultural University Experimental Field, Wuhan, China). The sample was pulverized and ground to a range of 0.075 mm to 0.250 mm as an experimental sample, and the sample was dried at 105 °C for 24 h. The relevant data from the RH proximate analysis and ultimate analysis are shown in Table 1. The neutral Al_2O_3 with a particle size of 1 mm to 2 mm was heated in a muffle furnace at 800 °C for 3 h and after self-cooling it was used again. The neutral Al_2O_3 with a particle size of 0.150 mm to 0.250 mm (analytical purity, National Pharmaceutical Group Chemical Reagent Co., Ltd., Shanghai, China) was dried at 105 °C for 24 h and cooling standby.

Table 1. Proximate Analysis, Ultimate Analysis, and LHV of Samples

Sample	Proximate Analysis (wt% ad)				Ultimate Analysis (wt% daf)					LHV (MJ/kg)
	M	V	A	FC	C	H	O[a]	N	S	
RH	8.03	67.20	9.66	15.11	55.19	6.93	37.08	0.35	0.46	17.884

Note: ad- air dry basis; daf- dry ash-free basis; M- moisture; V- volatile matter; A- ash; and FC- fixed carbon; [a] Calculated by difference

Methods

During the experiment, the (1 ± 0.1) g RH sample was mixed with Al_2O_3 (RH/Al_2O_3) in various ratios (1:5, 1:10, 1:15, and 1:20), in a blending manner (RH-B) and in a covering manner (RH-C). It was then placed in a porcelain boat and uniformly flattened (RH-B was low bulk density; RH-C was high bulk density). The RH/Al_2O_3 pyrolysis experiment was conducted in a tubular electric furnace (Yongguangming Medical Instrument Co., Ltd., Beijing, China). The main components were quartz tube fixed reaction beds with an inner diameter of 70 mm and a length of approximately 1000 mm. The porcelain boat loaded with the sample was placed in the low temperature area of the reactor, and 1 L/min of high-purity N_2 was added into the pyrolysis system to remove the O_2 in the reactor. The electric heating furnace was simultaneously opened to preheat the reactor. After the reactor temperature reached 600 °C, 1 L/min of high purity N_2 continued to pass through the system, and the porcelain boat was quickly moved to the center of the heating zone before timing began. After a certain time *t*, the boat was quickly removed from the heating zone and cooled in the N_2 condition. After the boat was completely cooled, it was weighed and placed it in a desiccator. The RH char and Al_2O_3 were separated and the RH char was stored in a sample bag. The weight loss of RH during rapid pyrolysis was observed through many experiments. It was finally determined that the holding time of the porcelain boat in the quartz tube reactor was 2 min to 6 min, and the prepared pyrolysis char was labeled as RH-B-t and RH-C-t. The structural analysis of char was obtained by pyrolysis of a 1:10 mixed sample (RH/Al_2O_3) and repeated for a total of three times.

Analysis instruments

Both thermogravimetric (TG) and differential thermogravimetric (DTG) curves were measured using a SDTQ600 TA synchronous thermal analyzer (TA instruments, New Castle, DE, USA). At the same time, a Fourier transform infrared spectrometer (FTIR, Thermo Scientific Nicolet iS50, Thermo Fisher Scientific, Shanghai, China) was used to monitor evolutionary gas fractions online. The pyrolysis process involved a 5 mg sample that was placed in a crucible and heated from room temperature to 900 °C at a heating rate of 20 °C/min in a N_2 atmosphere. The gas flow rate was maintained at 0.1 L/min. The gas products were recorded every 4 s. The FTIR was also used to analyze the chemical structure of the solids. The sample/KBr was thoroughly mixed and ground at a ratio of 1:150 (mass ratio) and pressed into a sheet with a diameter of approximately 5 mm for infrared analysis. The obtained spectrals were deducted from the pure KBr background, the infrared scanning wavelength range was 4000 cm^{-1} to 400 cm^{-1}, the resolution was 4 cm^{-1}. A D8 Advance X-ray diffractometer (Bruker, Karlsruhe, Germany) were used for the characterization of char crystal structure. The test conditions were: Cu target, Kα radiation; X-ray tube voltage: 40 kV; and X-ray tube current: 40 mA. Sample crystallite structure testing was performed over a 2θ angle range of 5° to 85°. The specific surface area and pore structure parameters were determined on the Micromerities ASAP 2020 (Micromeritics Instruments Corporation, Norcross, GA, USA) series of fully automatic static chemisorbers. The combustion experiment was performed using the SDTQ600 TA synchronous thermal analyzer. In an air atmosphere, a 5 mg sample was placed in a crucible and heated from room temperature to 900 °C at a heating rate of 20 °C /min, and the gas flow rate was maintained at 0.1 L/min.

Characteristic parameters

In this study, X-ray diffraction (XRD) analysis was an important means of analyzing the crystallinity and aromatic layers, which affect the combustion reactivity of char. The crystallites of RH char are superposed by several layers of aromatic layers (reference coal). The Bragg equation and the Scherrer formula were used for calculation. Because the structure of char is similar to coal, the calculation method of coal structure was referenced (López *et al.* 2013). The distance between the monolayers of the aromatic layer is indicated by d_{002}; the average stacking thickness (crystallite height) of each microcrystalline layer is indicated by L_{c}. The formula for calculating the above parameters is as follows,

$$d_{002} = \frac{1.5406}{2sin(\theta_{002})} \tag{1}$$

$$L_c = \frac{0.89 \times 1.5406}{\beta_{(002)} \cdot \cos(\theta_{002})} \tag{2}$$

where λ represents the wavelength of the X-ray (λ = 0.15406 nm), $\theta_{(002)}$is the diffraction angle corresponding to the peak position of the 002 peak, and $\beta_{(002)}$ is the half width value corresponding to the 002 peak.

To evaluate the combustion performance of bio-char under various conditions, the comprehensive combustibility index *S* was defined as follows (Yi *et al.* 2018a,b; Zhu *et al.* 2018),

$$S = \frac{(\mathrm{d}w/\mathrm{d}t)_{\mathrm{max}} \times (\mathrm{d}w/\mathrm{d}t)_{\mathrm{av}}}{T_{\mathrm{i}}^2 \times T_{\mathrm{b}}} \tag{3}$$

where $(\mathrm{d}w/\mathrm{d}t)_{\mathrm{max}}$ is the maximum combustion rate (%/min), $(\mathrm{d}w/\mathrm{d}t)_{\mathrm{av}}$ is the average weight loss rate (%/min), T_i (K) is the ignition temperature, and T_{b} is the burnout temperature (K). All of these were obtained through thermal gravimetric curves using the methods outlined in previous literature (Wang *et al.* 2012). Generally, a higher *S* value indicated a higher reactivity of the fuel combustion process.

RESULTS AND DISCUSSION

Conversion Rate of RH at Different Holding Times

The RH conversion rate resulted from different stacking ratios obtained at a constant temperature of 600 °C in a tube furnace. It was found that the increase in the accumulation ratio seriously affected heat transfer of the RH pyrolysis stage, considering the accumulation ratio has requirements for the pyrolysis process. Therefore, the RH sample and Al_2O_3 were mixed with in a ratio of 1:10. The RH char was prepared at a constant temperature of 600 °C and repeated three times at different holding times to investigate the RH char structure at each reaction stage. Figure 1 shows the RH conversion rate with the holding time. The holding time of less than 4 min can be defined as the volatile phase release stage and holding times greater than or equal to 4 min can be defined as the carbonization stage.

Figure 1 shows that the low bulk density was higher than the high bulk density conversion rate in each reaction stage. Moreover, the distances of the conversion rate curves of the two bulk densities first increased and then decreased. This indicated that the bulk density had a noticeable effect on the stage of volatilization release in the pyrolysis process, and the high bulk density hindered the heat transfer between the particles at this stage, which resulted in a lower release of volatiles from RH and low conversion rate. When the holding time increased, the temperature increased between the particles and the pyrolysis residue reached the release temperature of the volatiles, which weakened the influence of the bulk density on the carbonization stage. However, the low bulk density was still higher than the high bulk density conversion rate, which was due to the low bulk density. The RH particles were dispersed between the Al_2O_3 particles, which increased the diffusion rate of the volatiles on the surface of the particles. When the hot volatiles flowed through the surface of the cold particles, the convective heat transfer capacity was increased, so the pyrolysis reaction process was faster at low bulk density.

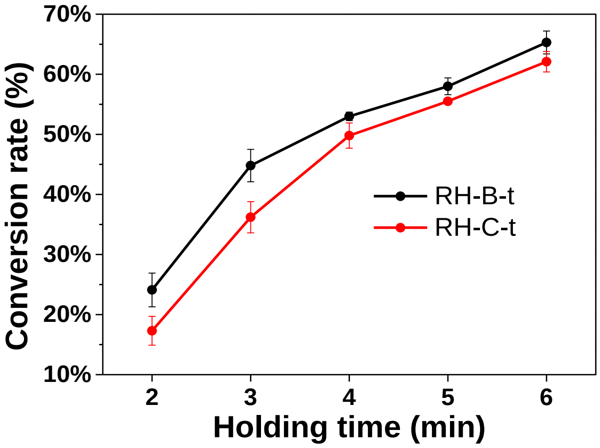

Fig. 1. Conversion rate of different RH bulk densities with increasing holding time

TG-FTIR Analysis

The thermogravimetric-infrared spectroscopy (TG-FTIR) technique was used to study the release of gas phase products during the pyrolysis of RH at different bulk densities. Fine particles of RH/Al_2O_3 were mixed at a ratio of 1:10. Figure 2 shows the TG and DTG curves using the conversion rate as an ordinate. According to Raveendran *et al.* (1996) and Almeida *et al.* (2019), the RH pyrolysis behavior occurs in a specific temperature range, and the initial part (200 °C to 320 °C) involves pyrolysis of semi-volatile substances. The latter (320 °C to 420 °C) can be attributed to pyrolysis of volatile compounds. Moreover, there was an additional loss in the range of 420 °C to 700 °C. A good separation process is shown on the DTG curve. Hemicellulose decomposition occurred at approximately 294 °C, cellulose decomposition occurred at approximately 345 °C, and the extra loss was the loss of residual carbon (Yang *et al.* 2007). The TG curves could be similarly divided into three stages under different bulk densities, namely the loss stage of moisture and more volatile matter, the loss stage of volatile compounds, and the stage of residual carbon loss.

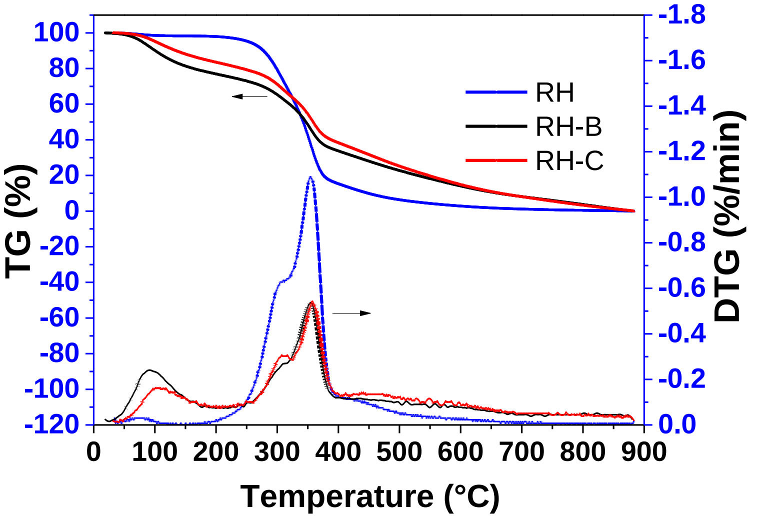

Fig. 2. The TG and DTG curves of RH, RH-B, and RH-C

The TG curves under the two bulk densities were gradually shifted to the low temperature region before 330 °C, while the offset at high bulk density was small. This may have been because the addition of Al_2O_3 increased the heat transfer capacity between the particles, while the high bulk density hindered the heat transfer between the RH particles compared to the low bulk density, resulting in a small offset. When the pyrolysis temperature increased, the distance between the TG curves under the two bulk densities first increased and then decreased. After 330 °C, the components of RH reached the main pyrolysis temperature range, and the blocking effect of the different bulk densities on pyrolysis gradually weakened. After 600 °C, the two TG curves tended to be consistent. This is due to the high temperature, the release of volatile substances in RH at different bulk densities is complete, and the temperature between the particles gradually tends to be the same, which results in consistent weight loss of residual char particles. Overall, the low bulk density condition pyrolysis reaction progressed faster than the high bulk density condition. This was similar to the conclusion of the tube furnace experiment. Moreover, the pyrolysis parameters of the DTG curve under the bulk density changed; for example, the maximum weight loss rate was lowered, and the temperature at which the pyrolysis ended moved to the high temperature region.

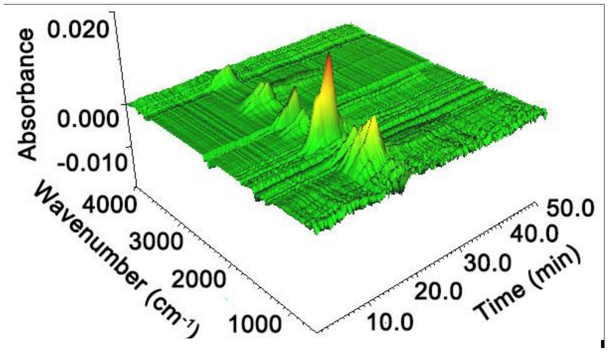

(a) RH

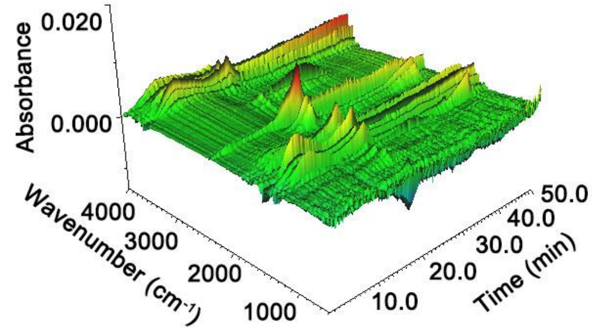

(b) RH-B

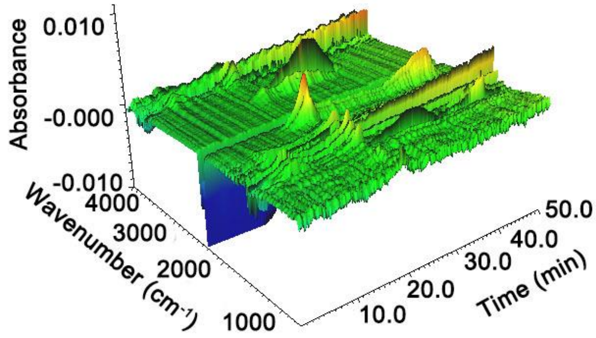

(c) RH-C

Fig. 3. FTIR three-dimensional spectrum of the gaseous pyrolysis compound of RH, RH-B, and RH-C in pyrolysis environment

Figure 3 shows that the gaseous products of the pyrolysis of RH and RH/Al_2O_3 samples were similar. According to the spectrum, it can be judged that the gaseous compound with wavenumbers of 3743 cm^{-1} and 1508 cm^{-1} was a characteristic peak of H_2O. The wavenumbers 2310 cm^{-1} and 2390 cm^{-1} represented a characteristic peak of CO_2. The wavenumbers 2112 cm^{-1} and 2181 cm^{-1} represented a characteristic peak of CO. The saturated and unsaturated hydrocarbon-based absorption peaks of 3000 cm^{-1} to 2850 cm^{-1} showed that there are many saturated hydrocarbons and unsaturated hydrocarbons in the product. The absorption characteristic peak of CH_4 is at 2870 cm^{-1} and 1460 cm^{-1} (Tahmasebi *et al.* 2012). The characteristic peaks of RH pyrolysis gaseous products were mainly concentrated in the time range of the volatiles release temperature range. The peak intensity of the gaseous products of the RH-B and RH-C samples decreased, and the peak intensity of the gaseous products of RH-C decreased more noticeably and no release of

CO_2 was detected. This indicated that the bulk density seriously affected the release rate and product distribution of gaseous substances.

FTIR Analysis

The FTIR analysis was performed to study the effect of different bulk densities on RH char structure during pyrolysis. Figure 4 shows the FTIR spectrum of RH char and RH prepared at a holding time of 2 min to 6 min. As the pyrolysis reaction progressed, the chemical structure of the RH char at each reaction stage showed a similar evolution. The main organic functional groups in RH and RH char were the hydroxyl bond (-OH, 3200 cm^{-1} to 3700 cm^{-1}), aliphatic bond (C-H, 2800 cm^{-1} to 3000 cm^{-1}), carbonyl bond (C=O, 1650 cm^{-1} to 1770 cm^{-1}), aromatic bond (C=C, 1450 cm^{-1} to 1600 cm^{-1}), ether bond (C-O-C, 1000 cm^{-1} to 1350 cm^{-1}), *etc.*, and the derivatives of these groups (Ma *et al.* 2018).

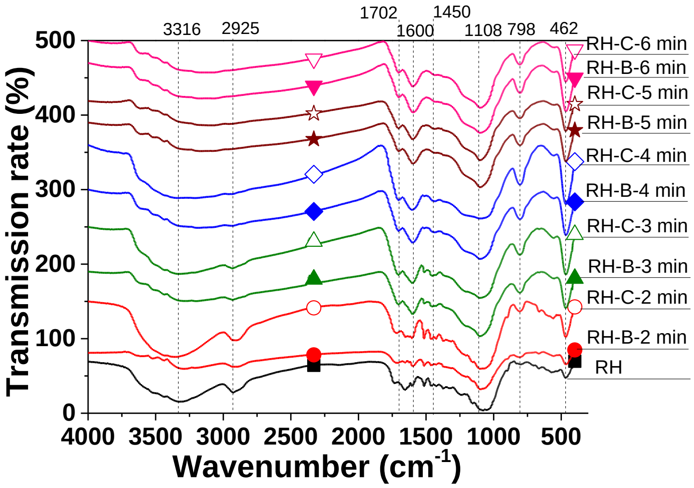

Fig. 4. FTIR spectrum of RH and RH char under various holding time

Figure 4 shows the attribution of the infrared absorption peak of RH char. The -OH and the C-H gradually disappeared, and the aromatic C=C and the oxygen-containing functional groups, such as C=O and C-O-C, tended to first increase and then decrease. At the same holding time, the low bulk density char and the -OH absorption band spectrum was wider and gentler. The absorption vibration peak of the C-H bond in char (RH-B- 2 min) was weaker than the absorption vibration peak of C-H bond in rice husk (RH). Due to the increase of holding time, the pyrolysis temperature increased, and the C-H bond in char (RH-B-4 min) basically cracked into a gaseous product, and the absorption vibration peak of the C-H bond basically disappeared. The aromatic C=C bond of the char (RH-C-3 min) began to develop. Shafizadeh and Sekiguchi (1983) found that the aromatic structure in cellulose char develops between 400 °C and 600 °C. The decrease of the H/C atomic ratio and the condensation and growth of the aromatic structure showed that the aromatization reaction was ongoing. In the char at the initial stage of carbonization, the aromatic C=C bond absorption peak reached a peak. However, in the char spectrum in the middle and late stages of carbonization, the aromatic C=C bond absorption vibration peak of the aromatic structure was weakened, which was caused by further carbonization reactions leading to benzene ring consumption (Almeida *et al.* 2019). Comparing the char FTIR spectrum at two bulk densities, in the release phase of volatiles, the loss of H and O in char prepared at low bulk density was faster, and the aromatic structure slowly increased. In the carbonization stage, the degree of aromatization in char was higher; however, the aromatic structure in the later stage of carbonization was gradually reduced.

X-ray Diffraction Analysis

Figure 5 shows the XRD diffraction patterns of RH and RH char prepared at different holding times. The RH had an obvious cellulose d_{101} crystal plane diffraction peak (also called γ band) between 10° and 18°, which was caused by the aliphatic side chain. Hemicellulose had diffraction peaks at 18° to 25° (Fan *et al.* 2015; Jiang *et al.* 2019). However, after pyrolysis under a high temperature, the hemicellulose was cleaved, and the diffraction peak gradually weakened to become a wide-dispersion and gentle 002 diffraction peak.

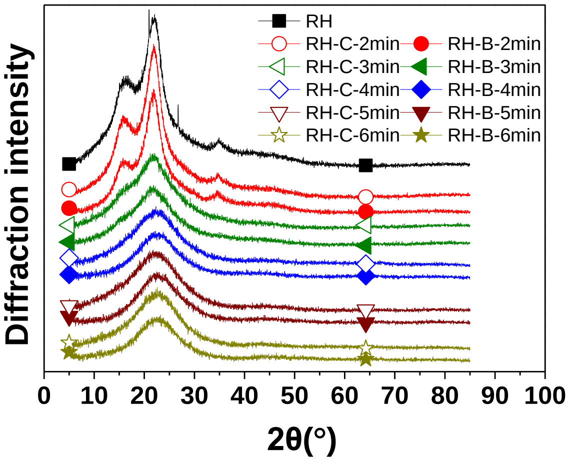

Fig. 5. XRD diffraction pattern of RH and RH char under various holding times

Compared with the RH, the γ diffraction peak of the aliphatic side chain structure disappeared in the char after the initial stage of volatiles released with the prolongation of the holding time. This indicated that an amorphous carbon structure occurred in the RH char in the middle stage of volatile matter release. In the carbonization stage, the char prepared at a high bulk density had a higher background intensity than that of the char prepared at a low bulk density. This means that the content of amorphous carbon produced by char at a high bulk density was higher. Cetin *et al.* (2004) showed that the 002 peak diffraction intensity indicated a high amorphous carbon content. At the same time, the 002 peak in the current study appeared at 22° and the 002 peak became more symmetrical and wider. These findings implied that the RH char had a highly disordered carbon structure. Figure 6 shows that the interlayer spacing d_{002} decreased with the increase of the holding time under the same bulk density, which indicated that the increase of the holding time had a noticeable effect on the change of the crystallite structure. However, the layer spacing d_{002} value of the char prepared at high bulk density was smaller, which may have been related to the decomposition of the aromatic structure during the pyrolysis of RH. The dense accumulation of particles hindered the release of gaseous products and the increase of pyrolysis pressure. However, the minimum value of the RH char microcrystalline lamellar spacing d_{002} was 0.392 nm, which was greater than the graphite layer spacing of 0.3354 nm. This meant that the char prepared at high bulk density was more prone to graphitization. However, considering the noticeable width, it could not be considered as the structure of the graphite crystal. Morin *et al.* (2016) evaluated the char structure of biomass that underwent rapid pyrolysis at 850 °C and found that the char contained some ordered structure attributable to the aromatic ring. The size of the aromatic ring was close to that of the graphite structure but cannot be considered as graphite considering the noticeable width. The stacking height L_c of the RH char aroma layer decreased with the increase of the holding time, which may have been the result of the addition of Al_2O_3 particles. However, the char stacking height L_c value prepared at high bulk density was larger, which meant that the char prepared at a high bulk density had a larger crystallite size. This indicated that the addition of Al_2O_3 limited the growth of aromatic crystallites, but high bulk density conditions hindered this limitation.

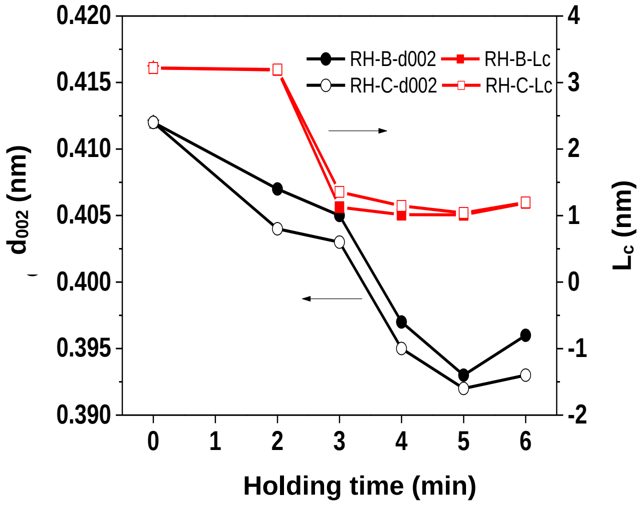

Fig. 6. Crystallite structure parameters of RH and RH char under various holding times

Pore Structure Analysis of RH and RH Char

The pore structure parameters of RH and RH char are shown in Table 2. The specific surface area of the RH was 0.556 m^2/g. Following pyrolysis carbonization, the specific surface area of the four RH chars was noticeably higher than that of the RH, especially the chars that underwent pyrolysis under low bulk density conditions. Moreover, the specific surface area of the four RH chars was two orders of magnitude larger than that of the RH samples. This indicated that the increase in surface area of RH under a N_2 atmosphere was related to changes in char conversion.

Table 2. Pore Structure Parameters of RH and RH Char

Sample	RH	RH-C-2 min	RH-B-2 min	RH-C-6 min	RH-B-6 min
Specific Surface Area (m^2/g)	0.556	15.429	17.440	21.746	29.703
Pore Volume (cm^3/g)	0.005	0.033	0.042	0.066	0.107
Pore Size (nm)	27.144	12.970	10.590	3.975	3.484

The low bulk density was due to the ease of heat transfer decomposition between the particles, and the release of volatiles led to an increasingly developed pore structure and thus a greater contribution to the surface area. The change in pore volume had a similar trend to the surface area, and the corresponding pore volume was also noticeably increased. However, the increase in char pore volume was less than the increase in surface area. In general, as the reaction progressed, the pore structure of char was complicated, and the specific surface area of microporous and mesoporous contribution with a pore diameter of less than 20 nm accounted for the majority of the specific surface area of raw RH and RH char. In the same reaction stage, the surface area and pore volume of the char sample prepared at high bulk density were smaller than the surface area and pore volume of char at low bulk density, because high bulk density conditions hindered particle heat transfer, moisture, and volatile release, which resulted in the small specific area and pore volume.

Combustion Reactivity of RH and RH Char

Figure 7 shows the change in the *S* of RH and RH char. The changes of *S* under different bulk densities were similar. As the holding time increased, the value of *S* gradually decreased. Also, there were fluctuations in the carbonization stage. Overall, the *S* of char prepared under high bulk density was higher than that of char prepared under low bulk density, especially in the volatile release stage.

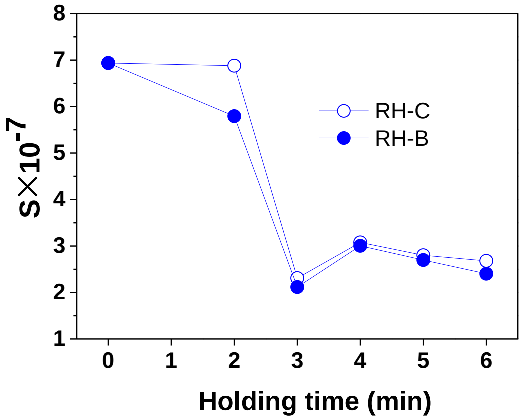

Fig. 7. S of RH and RH char under various holding times

The combustion performance of char was closely related to the volatile matter content, fixed carbon content, and pore structure. At the initial stage of volatiles release, it was apparent that the char prepared at high bulk density had better reactivity, which can be explained by the higher H and O contents in the carbon, which indicated the presence of -OH, C-H, and C=O in the char. According to Morin *et al.* (2016), the high content of these functional groups can strongly increase the oxidation reactivity of carbon. The reactivity of the char in the middle stage of volatile matter was reduced to the lowest point, which was an increase in the pyrolysis temperature, and the H and O contents in the char were reduced, and the functional groups, such as -OH and C=O, were destroyed to cause a decrease in reactivity. However, the reactivity of char at high bulk density was still slightly higher, which was the result of higher levels of C-H and amorphous carbon in the char at a high bulk density. Laurendeau (1978) studied the crosslink between C-H and amorphous carbons, which have weaker energy and are more susceptible to cleavage, which results in higher reactivity of char prepared at a high bulk density. The char reactivity in the carbonization stage was improved, but the reactivity of char was still much lower than that of char prepared at the initial stage of volatile release, and the char reactivity at different bulk densities was quite close. This was because the release of volatile products led to the development of a more disordered carbon structure and extensive pore structure. This increased the affinity of char with oxygen and increased reactivity. However, the aromatic C=C of the char at the initial stage of carbonization peaked, which led to the ordering of the molecular structure and the reduction of carbon edges and defects, the decrease in the number of active sites, and the decrease in reactivity. It was apparent that the increased degree of aromatization of char itself had a greater impact on reducing the reactivity. In the later stage of carbonization, the decrease in char reactivity was caused by a decrease in the amount of fixed carbon in the char. In summary, the increase in the aromaticity of carbon led to a decrease in reactivity, but the high bulk density hindered the pyrolysis process of RH, which resulted in higher residual volatiles and fixed carbon in the char prepared in the same reaction stage. Therefore, char prepared at a high bulk density had better combustion reactivity.

CONCLUSIONS

1. The bulk density of the particles affected the release rate and product distribution of gaseous products during pyrolysis, and the effect on the release stage of pyrolysis volatiles was particularly prominent. In comparison, the biomass pyrolysis carbonization process was faster under low bulk density conditions.
2. Comparing the pyrolysis at two bulk densities, pyrolysis of the particles at low bulk density resulted in a faster decrease in O and H content in RH, but a slower increase in aromatic structure. In the carbonization stage, low bulk density conditions promoted the increase in the surface area of char and expansion of pore volume, with a higher degree of aromatization. The addition of Al_2O_3 limited the growth of aromatic crystallites, but high bulk density conditions hindered this limitation. The char obtained at high bulk density tended to be graphitized.
3. The bulk density had a more pronounced effect on the reactivity of char in the volatiles release stage, but the effect on the reactivity of char in the carbonization stage was weakened. The reactivity of char prepared at different bulk densities showed a tendency to decrease. The char prepared at a high bulk density had better combustion reactivity.

ACKNOWLEDGMENTS

This research was primarily supported by Special Fund for Agro-Scientific Research in the public interest (201503135-11).

REFERENCES CITED

Almeida, S. R., Elicker, C., Vieira, B. M., Cabral, T. H., Silva, A. F., Sanches Filho, P. J., Raubach, C. W., Hartwig, C. A., Mesko, M. F., Moreira, M. L., *et al.* (2019). "Black SiO_2 nanoparticles obtained by pyrolysis of rice husk," *Dyes and Pigments* 164, 272-278. DOI: 10.1016/j.dyepig.2019.01.030

Atreya, A., Olszewski, P., Chen, Y., and Baum, H. R. (2017). "The effect of size, shape and pyrolysis conditions on the thermal decomposition of wood particles and firebrands," *International Journal of Heat and Mass Transfer* 107, 319-328. DOI: 10.1016/j.ijheatmasstransfer.2016.11.051

Azuara, M., Fonts, I., Bimbela, F., Murillo, M. B., and Gea, G. (2015). "Catalytic post-treatment of the vapors from sewage sludge pyrolysis by means of γ-Al_2O_3: Effect on the liquid product properties," *Fuel Processing Technology* 130, 252-262. DOI: 10.1016/j.fuproc.2014.10.014

Biagini, E., Simone, M., and Tognotti, L. (2009). "Characterization of high heating rate chars of biomass fuels," *Proceedings of the Combustion Institute* 32(2), 2043-2050. DOI: 10.1016/j.proci.2008.06.076

Burhenne, L., Damiani, M., and Aicher, T. (2013). "Effect of feedstock water content and pyrolysis temperature on the structure and reactivity of spruce wood char produced in fixed bed pyrolysis," *Fuel* 107, 836-847. DOI: 10.1016/j.fuel.2013.01.033

Cataldo, S., Chiodo, V., Crea, F., Maisano, S., Milea, D., and Pettignano, A. (2018). "Biochar from byproduct to high value added material – A new adsorbent for toxic metal ions removal from aqueous solutions," *Journal of Molecular Liquids* 271, 481-489. DOI: 10.1016/j.molliq.2018.09.009

Cetin, E., Moghtaderi, B., Gupta, R., and Wall, T. F. (2004). "Influence of pyrolysis conditions on the structure and gasification reactivity of biomass chars," *Fuel* 83(16), 2139-2150. DOI: 10.1016/j.fuel.2004.05.008

Chandra, S., and Bhattacharya, J. (2019). "Influence of temperature and duration of pyrolysis on the property heterogeneity of rice straw biochar and optimization of pyrolysis conditions for its application in soils 430/5000," *Journal of Cleaner Production* 215, 1123-1139. DOI: 10.1016/j.jclepro.2019.01.079

Fan, C., Yan, J., Huang, Y., Han, X., and Jiang, X. (2015). "XRD and TG-FTIR study of the effect of mineral matrix on the pyrolysis and combustion of organic matter in shale char," *Fuel* 139, 502-510. DOI: 10.1016/j.fuel.2014.09.021

Jian, J., Lu, Z., Yao, S., Li, Y., Liu, Z., Lang, B., and Chen, Z. (2019). "Effects of thermal conditions on char yield and char reactivity of woody biomass in stepwise pyrolysis," *Journal of Analytical and Applied Pyrolysis* 138, 211-217. DOI: 10.1016/j.jaap.2018.12.026

Jiang, J., Yang, W., Cheng, Y., Liu, Z., Zhang, Q., and Zhao, K. (2019). "Molecular structure characterization of middle-high rank coal *via* XRD, Raman and FTIR spectroscopy: Implications for coalification," *Fuel* 239, 559-572. DOI: 10.1016/j.fuel.2018.11.057

Klinger, J. L., Westover, T. L., Emerson, R. M., Williams, C. L., Hernandez, S., Monson, G. D., and Ryan, J. C. (2018). "Effect of biomass type, heating rate, and sample size on microwave-enhanced fast pyrolysis product yields and qualities," *Applied Energy* 228, 535-545. DOI: 10.1016/j.apenergy.2018.06.107

Lateef, A., Nazir, R., Jamil, N., Alam, S., Shah, R., Khan, M. N., Saleem, M., and Rehman, S.-U. (2019)."Synthesis and characterization of environmental friendly corncob biochar based nano-composite – A potential slow release nano-fertilizer for sustainable agriculture," *Environmental Nanotechnology, Monitoring & Management* 11, 100212. DOI: 10.1016/j.enmm.2019.100212

Laurendeau, N. M. (1978). "Heterogeneous kinetics of coal char gasification and combustion," *Progress in Energy and Combustion Science* 4(4), 221-270. DOI: 10.1016/0360-1285(78)90008-4

López, F. A., Centeno, T. A., García-Díaz, I., and Alguacil, F. J. (2013). "Textural and fuel characteristics of the chars produced by the pyrolysis of waste wood, and the properties of activated carbons prepared from them," *Journal of Analytical and Applied Pyrolysis* 104, 551-558. DOI: 10.1016/j.jaap.2013.05.014

Ma, Z., Wang, J., Yang, Y., Zhang, Y., Zhao, C., Yu, Y., and Wang, S. (2018). "Comparison of the thermal degradation behaviors and kinetics of palm oil waste under nitrogen and air atmosphere in TGA-FTIR with a complementary use of model-free and model-fitting approaches," *Journal of Analytical and Applied Pyrolysis* 134, 12-24. DOI: 10.1016/j.jaap.2018.04.002

Morin, M., Pécate, S., Hémati, M., and Kara, Y. (2016). "Pyrolysis of biomass in a batch fluidized bed reactor: Effect of the pyrolysis conditions and the nature of the biomass on the physicochemical properties and the reactivity of char," *Journal of Analytical and Applied Pyrolysis* 122, 511-523. DOI: 10.1016/j.jaap.2016.10.002

Pehlivan, E., Özbay, N., Yargıç, A. S., and Şahin, R. Z. (2017). "Production and characterization of chars from cherry pulp *via* pyrolysis," *Journal of Environmental Management* 203(Part 3), 1017-1025. DOI: 10.1016/j.jenvman.2017.05.002

Pimenta, A. S., Monteiro, T. V. d. C., Fasciotti, M., Braga, R. M., De Souza, E. C., and De Lima, K. M. G. (2018). "Fast pyrolysis of trunk wood and stump wood from a Brazilian eucalyptus clone," *Industrial Crops and Products* 125, 630-638. DOI: 10.1016/j.indcrop.2018.08.083

Raveendran, K., Ganesh, A., and Khilar, K. C. (1996). "Pyrolysis characteristics of biomass and biomass components," *Fuel* 75(8), 987-998. DOI: 10.1016/0016-2361(96)00030-0

Rizzo, A. M., Pettorali, M., Nistri, R., and Chiaramonti, D. (2019). "Mass and energy balances of an autothermal pilot carbonization unit," *Biomass and Bioenergy* 120, 144-155. DOI: 10.1016/j.biombioe.2018.11.009

Shafizadeh, F., and Sekiguchi, Y. (1983). "Development of aromaticity in cellulosic chars," *Carbon* 21(5), 511-516. DOI: 10.1016/0008-6223(83)90144-6

Tahmasebi, A., Yu, J., Han, Y., and Li, X. (2012). "A study of chemical structure changes of Chinese lignite during fluidized-bed drying in nitrogen and air," *Fuel Processing Technology* 101, 85-93. DOI: 10.1016/j.fuproc.2012.04.005

Thines, K. R., Abdullah, E. C., and Mubarak, N. M. (2017). "Effect of process parameters for production of microporous magnetic biochar derived from agriculture waste biomass," *Microporous and Mesoporous Materials* 253, 29-39. DOI: 10.1016/j.micromeso.2017.06.031

Wang, C., Zhang, X., Liu, Y., and Che, D. (2012). "Pyrolysis and combustion characteristics of coals in oxyfuel combustion," *Applied Energy* 97, 264-273. DOI: 10.1016/j.apenergy.2012.02.011

Yang, H., Yan, R., Chen, H., Lee, D. H., and Zheng, C. (2007). "Characteristics of hemicellulose, cellulose and lignin pyrolysis," *Fuel* 86(12-13), 1781-1788. DOI: 10.1016/j.fuel.2006.12.013

Yi, B., Yuan, Q., Cao, H., Wang, M., Niu, W., and Yan, S. (2018a). "Combustion characteristics of densified cattle manure briquette in an isothermal condition," *BioResources* 13(2), 3571-3584. DOI: 10.15376/biores.13.2.3571-3584

Yi, B., Zhang, L., and Yuan, Q. (2018b). "Study of the flue gas characteristics and gasification reaction of pulverized coal combustion in $O_2/CO_2/H_2O$ atmosphere," *Energy Sources Part A: Recovery, Utilization, and Environmental Effects* 40(13), 1565-1572. DOI: 10.1080/15567036.2018.1477870

Yi, B., Zhang, L.-Q., Yuan, Q.-X., Yan, S.-P., and Zheng, C.-G. (2016). "The evolution of coal char structure under the oxy-fuel combustion containing high H_2O," *Fuel Processing Technology* 152, 294-302. DOI: 10.1016/j.fuproc.2016.06.017

Zhao, B., O'Connor, D., Zhang, J., Peng, T., Shen, Z., Tsang, D. C. W., and Hou, D. (2018). "Effect of pyrolysis temperature, heating rate, and residence time on rapeseed stem derived biochar," *Journal of Cleaner Production* 174, 977-987. DOI: 10.1016/j.jclepro.2017.11.013

Zhu, Y., Yi, B., Yuan, Q., Cao, H., and Yan, S. (2018). "Combustion characteristics of cattle manure and pulverized coal co-firing under oxy-fuel atmosphere in non-isothermal and isothermal conditions," *BioResources* 13(3), 6465-6479. DOI: 10.15376/biores.13.3.6465-6479

Article submitted: May 21, 2019; Peer review completed: August 4, 2019; Revised version received: August 5, 2019; Accepted: August 27, 2019; Published: August 30, 2019.
DOI: 10.15376/biores.14.4.8289-8303